Kupletskite polytypes from the Lovozero massif, Kola Peninsula, Russia: Kupletskite-1A kupletskite-Ma2b2c

Article *in* European Journal of Mineralogy · September 2001

DOI: 10.1127/0935-1221/2001/0013/0973

CITATIONS
25

READS
42

3 authors, including:

Paula Piilonen
Canadian Museum of Nature
42 PUBLICATIONS **359** CITATIONS

SEE PROFILE

Andy Mcdonald
Laurentian University
91 PUBLICATIONS **991** CITATIONS

SEE PROFILE

Eur. J. Mineral.
2001, **13**, 973–984

Kupletskite polytypes from the Lovozero massif, Kola Peninsula, Russia: Kupletskite-1A and kupletskite-Ma2b2c

PAULA C. PIILONEN[1], ANDREW M. McDONALD[2] and ANDRÉ E. LALONDE[1]

[1]Ottawa-Carleton Geoscience Centre, Department of Earth Sciences,
University of Ottawa, Ottawa, Ontario K1N 6N5, Canada
e-mail: ppiilon@science.uottawa.ca
[2]Department of Earth Sciences, Laurentian University, Sudbury, Ontario P3E 2C6, Canada

Abstract: The crystal structures of two kupletskite [$K_2NaMn_7Ti_2Si_8O_{26}(OH)_4F$] polytypes, (1) triclinic, space group $P\overline{1}$, and (2) monoclinic, space group $C2/c$, from nepheline syenite pegmatites of the Lovozero massif, Russia, have been determined. The two structures differ in the stacking sequence of an identical *HOH* layer (where *H* = heterophyllosilicate and *O* = octahedral): in the triclinic structure, individual *HOH* layers are related by a centre of symmetry, resulting in a *+HOH/+HOH/+HOH* stacking sequence with a one-layer period; in monoclinic kupletskite, adjacent *HOH* layers are related by a two-fold axis parallel to *b*, resulting in a *+HOH/-HOH/+HOH* stacking sequence with a two-layer period. The resultant relationship between the unit cell parameters of monoclinic kupletskite-*Ma2b2c* and triclinic kupletskite-1*A* are as follows: $a_{monoclinic} = a_{triclinic}$, $b_{monoclinic} = 2(b\sin\gamma)_{triclinic}$, and $c_{monoclinic}$ spans two *HOH* layers. These results represent the first single-crystal X-ray structure determination of polytypes in the astrophyllite group.

Key-words: astrophyllite group, kupletskite, polytype, Lovozero, *HOH* layer.

Sommaire: Nous avons déterminé la structure cristalline de deux polytypes de kupletskite, un premier triclinique de symétrie spatiale $P\overline{1}$, et l'autre monoclinique, de symétrie spatiale $C2/c$, tous deux provenant des pegmatites de syénite à néphéline du massif Lovozero en Russie. Les deux structures se distinguent par leurs séquences d'empilements de couches *HOH* (où *H* = couche hétérophyllosilicatée et *O* = couche octaédrique): dans l'échantillon triclinique, les couches *HOH* individuelles sont reliées les unes aux autres par un centre de symétrie, produisant ainsi une séquence d'empilement du type *+HOH/+HOH/+HOH* ayant une périodicité d'une couche alors que dans l'exemple monoclinique, les couches *HOH* adjacentes sont reliées les unes aux autres par une rotation d'orde 2 parallèle à *b*, ce qui mène à une séquence d'empilement du type *+HOH/-HOH/+HOH* avec une périodicité de deux couches. La correspondance entre les paramètres du polytype monoclinique (kupletskite-*Ma2b2c*) et celui triclinique (kupletskite-1*A*) est la suivante: $a_{monoclinique} = a_{triclinique}$, $b_{monoclinique} = 2\ (b\sin\gamma)_{triclinique}$, et le paramètre $c_{monoclinique}$ s'étend sur deux couches *HOH*. Cette étude documente pour la première fois l'existence du polytypisme dans le groupe de l'astrophyllite par des méthodes de diffraction-X sur monocristaux.

Mots-clés: groupe de l'astrophyllite, kupletskite, polytype, Lovozero, couche *HOH*.

Introduction

Astrophyllite group minerals (AGM) are alkali titano-, niobo- and zirconosilicates which have the general formula $A_2BC_7D_2T_8O_{26}(OH)_4X_{0-1}$ where *A* = [10-13]K, Rb, Cs, Na, H_3O, H_2O, or □; *B* = [10]Na or Ca; *C* = [6]Mn, Fe^{2+}, Fe^{3+}, Na, Mg, or Zn; *D* = [6]Ti, Nb, or Zr; *T* = Si and Al, *X* = F, OH, O, or □ (Piilonen *et al.*, 2000). Kupletskite, ideally $K_2NaMn_7Ti_2Si_8O_{26}(OH)_4F$, one of eight known AGM, is found in SiO_2-oversaturated alkaline rocks such as Point of Rocks, New Mexico, USA

0935-1221/01/0013/0973 $ 3.00
DOI: 10.1127/0935-1221/2001/0013/0973

(DeMark, 1984), Gjerdingen, Norway (Raade & Haug, 1982), and the Junguni intrusion, Chilwa, Malawi (Woolley & Platt, 1988), and SiO_2-undersaturated intrusions such as the Lovozero massif, Kola Peninsula (Semenov, 1956) and the Azov region, Russia (Valter *et al*., 1965), the Larvik complex, Langesundsfjord area, Norway (Piilonen unpublished data), the Werner Bjerge complex and Kangerdlugssuaq, East Greenland (Brooks *et al*., 1982; Christiansen *et al*., 1998), and Mont Saint-Hilaire, Québec, Canada (Horváth & Gault, 1990; Piilonen *et al*., 2000).

Kupletskite was initially described by Semenov (1956) from nepheline syenite pegmatites in the Lepkhe-Nelm and Kuivchorr mountains of the Lovozero massif, Kola Peninsula, Russia. It occurs as coarse-grained (up to 0.5 cm), anhedral to subhedral, dark brown, platy to acicular crystals associated with aegirine, natrolite, eudialyte group minerals, microcline, mangano-pectolite, and neptunite. In the original description, no data pertaining to the space group or cell parameters were provided, and only monoclinic or triclinic (pseudomonoclinic) symmetry was proposed. Peng & Ma (1963) described a Mn-dominant astrophyllite from Russia with triclinic symmetry ($P\bar{1}$) but did not elaborate on its relationship with kupletskite. Christiansen *et al*. (1998) refined the structure of a kupletskite from Kangerdlugssuaq, east Greenland, and confirmed it to be triclinic, space group $P\bar{1}$. Structure analyses on holotype kupletskite from Mount Kuivchorr (Lovozero) and a sample from Lephke-Nelm were performed as part of a larger study on the crystal chemistry and paragenesis of members of the astrophyllite group. During data collection, the possibility of a monoclinic polytype was recognized and further analyses were performed.

Crystal structure analyses confirm kupletskite from Mount Kuivchorr to be triclinic, space group $P\bar{1}$, whereas that from Lephke-Nelm was found to be monoclinic, space group $C2/c$. The existence of two structural states for kupletskite is the result of polytypism in the astrophyllite group. The objectives of the following study are to: (1) describe and compare the crystal structures of triclinic and monoclinic kupletskite, (2) discuss the mechanism for polytype formation in AGM, and (3) to introduce polytype nomenclature into the astrophyllite group in accordance with the guidelines proposed by the IMA Commission on New Minerals and Mineral Names (Bailey *et al.*, 1978; Nickel & Grice, 1998).

Table 1. Chemical composions of triclinic (RUS12) and monoclinic (RUS9) kupletskite*.

	RUS12			RUS9		
Oxide	1	2	Ave.	1	2	Ave.
Na_2O	2.60	2.61	2.61	2.14	2.00	2.07
K_2O	5.90	5.92	5.91	6.16	6.25	6.21
Rb_2O	0.51	0.49	0.50	0.50	0.50	0.50
Cs_2O	0.00	0.00	0.00	0.00	0.05	0.03
CaO	1.37	1.38	1.38	1.24	1.30	1.27
SrO	0.25	0.20	0.23	0.29	0.24	0.27
BaO	0.00	0.13	0.07	0.55	0.48	0.52
MgO	1.96	1.92	1.94	1.38	1.45	1.42
MnO	27.55	27.50	27.53	21.47	21.44	21.46
FeO	4.11	4.15	4.13	10.91	11.05	10.98
Al_2O_3	0.23	0.25	0.24	1.00	1.08	1.04
Ce_2O_3	0.00	0.14	0.07	0.32	0.25	0.29
ZrO_2	0.00	0.00	0.00	0.00	0.00	0.00
TiO_2	11.45	11.35	11.40	10.31	10.72	10.52
Nb_2O_5	0.79	0.75	0.77	2.37	2.38	2.38
SiO_2	36.67	36.02	36.35	34.47	34.81	34.64
F	1.25	1.06	1.16	1.05	1.14	1.10
H_2O	2.82	2.87	2.85	2.83	2.83	2.83
O=F	–0.53	–0.45	–0.49	–0.44	–0.48	–0.46
Total	96.93	96.43	96.68	96.55	97.49	97.02
Formula based on 31 anions						
K	1.65	1.68	1.67	1.77	1.78	1.77
Rb	0.07	0.07	0.07	0.07	0.07	0.07
Cs	0.00	0.00	0.00	0.00	0.01	0.00
Sr	0.03	0.03	0.03	0.04	0.03	0.03
Ba	0.00	0.01	0.01	0.05	0.04	0.05
Na	0.00	0.04	0.02	0.00	0.00	0.00
Sum *A*	1.76	1.82	1.79	1.93	1.93	1.93
Na	0.63	0.67	0.65	0.58	0.46	0.52
Ca	0.32	0.33	0.33	0.30	0.31	0.31
Sum *B*	0.95	1.00	0.97	0.88	0.77	0.82
Na	0.48	0.41	0.44	0.36	0.40	0.38
Mg	0.64	0.64	0.64	0.46	0.48	0.47
Mn	5.13	5.17	5.15	4.10	4.04	4.07
Fe^{2+}	0.76	0.77	0.77	2.06	2.06	2.06
Ce	0.00	0.01	0.01	0.03	0.02	0.02
Sum *C*	7.01	7.00	7.00	7.00	7.00	7.00
Ti	1.89	1.90	1.90	1.75	1.80	1.78
Nb	0.08	0.08	0.08	0.24	0.24	0.24
Zr	0.00	0.00	0.00	0.00	0.00	0.00
Sum *D*	1.97	1.98	1.97	1.99	2.04	2.02
Si	8.05	8.00	8.03	7.77	7.75	7.76
Al	0.06	0.06	0.06	0.27	0.28	0.28
Sum *T*	8.11	8.06	8.09	8.04	8.03	8.04
F	0.87	0.74	0.81	0.75	0.80	0.78
OH	4.13	4.26	4.20	4.25	4.21	4.23
O	26.00	26.00	26.00	26.00	26.00	26.00
Σcat.	19.79	19.86	19.83	19.83	19.77	19.80

* Electron-microprobe data

Chemical composition

Two kupletskite samples were analysed: RUS9 (Lephke-Nelm) and RUS12 (holotype material, Mount Kuivchorr). Chemical analyses were performed on a JEOL 733 electron microprobe in wavelength-dispersive mode using Tracor Northern 5500 and 5600 automation software. Details regarding operating conditions and standard selection can be found in Piilonen *et al*. (2000). Complete electron microprobe data can be found in Table 1. Chemical formulae were calculated on the basis of 31 anions and 5(OH,F,O) as determined from the crystal structure analysis.

X-ray crystallography

X-ray powder diffraction data for RUS9 and RUS12 were collected with a 114.6 Debye-Scherrer camera employing Cu$K\alpha$ radiation (Ni-filtered) operating at 45 kV and 20 mA (24 hour exposure) and 40 kV and 30 mA (6 hour exposure), respectively. Observed and calculated (PowderCell, 1999) X-ray powder diffraction patterns for both polytypes are presented in Table 2. Monoclinic and triclinic kupletskite polytypes can be distinguished on the basis of their X-ray powder diffraction patterns in two main regions. The most evident difference between the two patterns is the presence of a moderately strong (I_{obs} = 30) peak at ~9.8 Å in triclinic modifications that is absent in monoclinic kupletskite. Secondly, in triclinic kupletskite, a broad band is observed between 30 and 40° 2θ (Cu$K\alpha$ radiation), corresponding to approximately ~2.656 Å. Close examination of this band reveals two separate peaks, spaced closely together at 2.659 and 2.648 Å. In monoclinic kupletskite, the splitting of these peaks is more pronounced and the two peaks easily resolved (2.661 and 2.634 Å).

Intensity data for both crystals were collected using the Siemens SMART system consisting of a four-circle goniometer and a 1 K (diameter: 9 cm, 512 x 512 pixel) charge-coupled device (CCD) area detector. Data were collected at room temperature using monochromatic Mo$K\alpha$ X-radiation, with the X-ray tube operating at 50 kV and 40 mA, and a fixed detector-crystal distance of 4 cm. A frame width (ω) of 0.2° and count exposure times of 45 s were used. Data collection consisted of 4349 frames, out to 2θ = 60°, which provided 100 % coverage of the diffraction sphere with a mean redundancy of 3.6 times. Approximately 1000 reflections with spot sizes of 2.4 ° (*XY*, in the plane) and 2.0° (*Z*, through the plane) were used in determination of the orientation matrix and preliminary unit cell prior to integration of all frames data. The data were reduced, filtered, integrated, and corrected for Lorentz, polarization and background effects using the Siemens software SAINT. Absorption corrections were performed using SADABS and crystals were modeled as an ellipse. All reflection data were then merged using the program XPREP (Bruker Analytical X-ray Systems, 1997). Information pertinent to the data collection and crystal structure can be found in Table 3.

The structure of RUS12 was refined using starting parameters taken from niobokupletskite (Piilonen *et al*., 2000), an isostructural AGM. Phasing of a set of normalized structure factors gave a mean $|E^2-1|$ of 1.071, suggesting $P\bar{1}$ as the most probable space group, consistent with data obtained for other triclinic astrophyllite group minerals (Peng & Ma, 1963; Woodrow, 1967; Christiansen *et al*., 1998; Piilonen *et al*., 2000). The structure refined to R = 5.26 % and wR^2 = 14.58 % with isotropic displacement factors and reduced to R = 4.06 % and wR^2 = 11.25 % with anisotropic displacement factors. An isotropic extinction correction was applied but did not improve the final residual. Initial site assignments were as follows: Mn to all four crystallographically distinct *M* sites [*M*(1) to *M*(4)], Ti to *D*, and Na to *B*. Refinement of the site occupancy factors included assigning Na to *M*(1), Mg to *M*(4), Nb to *D*, Si to *T*, and Ca to *B* and K to *A*, in accordance with the need for either a heavier or lighter X-ray scatterer at the given site, and in keeping with the electron microprobe data for the crystal. The shape of the anisotropic displacement ellipsoid of the K site suggested that the K cation was positionally disordered and it was therefore modeled as two split sites, *K*(1a) and *K*(1b), displaced 0.917 Å from each other in the (001) plane. Displacement factors for *K*(1a) and *K*(1b) were constrained to be equal and refined isotropically. The final positional and isotropic displacement parameters are given in Table 4. Bond valence sums were calculated using parameters taken from Brese & O'Keeffe (1991) and can be found in Table 5.

During unit cell and orientation matrix determination, it was noted that sample RUS9 gave a metrically monoclinic cell with *b* and *c* parameters approximately double with respect to those of the triclinic species ($b_{monoclinic}$ 23.226 Å *versus* $b_{triclinic}$ 11.9283 Å, $c_{monoclinic}$ 21.1782 Å *versus* $c_{triclinic}$ 11.7256 Å). Possible space groups included *Cc* and *C*2/*c*, with combined figures of merit of 32.58 and 11.92, respectively. Phasing of a set of normalized

Table 2. X-ray powder diffraction data for triclinic and monoclinic kupletskite.

Triclinic, kupletskite-1*A* *					Monoclinic, kupletskite-*Ma*2*b*2*c* **				
d_{meas}	d_{calc}	I_{obs}	I_{calc}	*hkl*	d_{meas}	d_{calc}	I_{obs}	I_{calc}	*hkl*
10.589	10.587	100	100	001	10.589	10.545	100	100	002
	10.529		30	010					
						10.173		45	021
9.853	9.828	30	23	$01\bar{1}$					
5.757	5.790	20	7	$02\bar{1}$	5.795	5.806	<5	8	040
					5.107	5.086	<5	<5	042
4.436	4.413	10	5	$\bar{1}\bar{1}1$	4.399	4.391	<5	5	$\bar{1}31$
4.338	4.348	7	<5	$12\bar{0}$		4.260		<5	131
4.111	4.110	<5	<5	$\bar{1}02$		3.903		5	044
3.763	3.757	<5	<5	$02\bar{3}$	3.897	3.894	<5	<5	$\bar{1}14$
3.713	3.717	10	5	$12\bar{2}$					
						3.620		14	133
3.528	3.529	40	27	003	3.522	3.515	40	30	006
	3.276		<5	$03\bar{3}$					
3.276		20			3.255	3.268	<5	<5	134
	3.272		9	$\bar{1}\bar{1}3$					
					3.170	3.172	<5	16	$\bar{1}35$
3.095	3.089	12	7	$\bar{1}22$	3.096	3.120	<5	<5	063
3.035	3.031	12	7	$12\bar{3}$	2.931	2.942	<5	8	135
2.861	2.862	5	<5	$13\bar{3}$	2.855	2.852	<5	<5	065
						2.847		6	154
2.820	2.820	<5	<5	121					
2.782	2.783	20	16	$\bar{1}\bar{3}1$	2.783	2.782	20	38	171
2.659	2.662	15	18	$\bar{2}11$	2.661	2.665	10	18	$\bar{2}02$
2.648	2.647	12	12	004					
					2.634	2.636	15	12	008
2.582	2.582	35	20	130	2.580	2.578	30	37	$\bar{1}73$
2.491	2.490	15	13	$\bar{2}12$	2.494	2.490	8	14	$\bar{2}04$
2.405	2.408	12	5	$\bar{1}41$	2.400	2.400	5	9	$\bar{1}75$
2.299	2.301	15	6	131	2.293	2.296	10	13	175
2.240	2.239	10	10	$\bar{2}13$	2.240	2.237	5	9	$\bar{2}06$
	2.120		<5	$\bar{1}42$					
	2.117		<5	005	2.110	2.112	15	7	$\bar{1}77$
2.114		15				2.109		<5	0.0.10
	2.113		<5	$\bar{1}\bar{3}5$					
2.045	2.047	5	6	$2\bar{1}3$	2.046	2.048	5	6	206
2.015	2.012	5	<5	$14\bar{5}$	2.010	2.013	<5	5	177
1.766	1.768	<5	5	133	1.761	1.762	12	12	179
1.743	1.743	<5	7	$\bar{2}15$	1.738	1.739	<5	7	$\bar{2}.0.10$
1.661	1.660	5	9	$07\bar{3}$	1.661	1.661	<5	<5	333
						1.659		9	0.14.0
1.629	1.630	<5	<5	$\bar{1}44$	1.624	1.623	<5	5	$\bar{1}.7.11$
1.582	1.581	<5	6	$3\bar{2}2$	1.584	1.583	<5	13	$\bar{3}71$
	1.581		6	$3\bar{5}1$					
					1.508	1.506	<5	<5	0.0.14
1.443	1.444	<5	<5	$\bar{1}45$	1.439	1.437	<5	<5	$\bar{1}.7.13$
1.412	1.415	<5	<5	$2\bar{1}6$	1.411	1.413	<5	<5	2.0.12

* 6 hour exposure. ** 24 hour exposure.

Cu*K* α radiation, Ni filtered, Debye-Scherrer camera 114.6 mm in radius, with intensities visually estimated. The values of *d* are expressed in Å.

Table 3. Miscellaneous data for kupletskite-1*A* and kupletskite-*Ma*2*b*2*c*.

Parameter	Kupletskite-1*A*	Kupletskite-*Ma*2*b*2*c*
Space Group	*P*	*C*2/*c*
a (Å)	5.3925(2)	5.4022(2)
b	11.9283(4)	23.226(1)
c	11.7256(4)	21.1782(9)
α (°)	113.044(1)	90
β	94.840(1)	95.246(1)
γ	103.064	90
V (Å^3)	663.39(7)	2646.2(3)
Z	1	4
Crystal morphology	plate flattened on {001}	
Crystal size (mm^3)	0.25x0.20x0.03	0.25x0.25x0.03
μ (Mo*K*α) cm^{-1}	4.30	4.94
Reflections collected	6813	13834
Unique reflections	3834	3865
R_{int} (%)	2.98	3.55
Min/Max Trans.	0.515/0.773	0.499/0.720
$\|E^2-1\|$	1.081	1.294
Min/Max Indices	$-7 \le h \le 7$	$-7 \le h \le 7$
	$-16 \le k \le 16$	$-32 \le k \le 32$
	$-16 \le l \le 16$	$-29 \le l \le 29$
Criterion for Observed Reflections $F_o>4\sigma(F_o)$		
Final *R* (%)	4.06	4.72
wR^2 (%)	11.25	14.04
Diffractometer parameters (for both data collections)		
Diffractometer	SIEMENS 4-circle CCD	
Radiation	Mo*K*α (40 kV, 30 mA)	
2θ Range (°)	$4.82 \le 2\theta \le 57.26$	

$R = \Sigma(|F_o|-|F_c|)/\Sigma|F_o|$
$wR^2 = [\Sigma(w)F_o^2 - F_c^2)^2/\Sigma[w(F_o^2)^2]^{1/2}$, $w = 1/\sigma^2(F_o)$

structure factors gave a mean $|E^2-1|$ of 1.294 suggesting the centrosymmetric space group *C*2/*c* as the most probable choice. The structure of monoclinic RUS9 was solved using direct methods in space group *C*2/c and further refined using the SHELXL-93 set of programs (Sheldrick, 1993). The positions of all major cations and 12 O^{2-} atoms were located on the *E*-map. The remaining cation and anion positions were located using difference Fourier maps during the refinement. The structure refined to *R* = 7.20 % and wR^2 = 19.99 % with isotropic displacement factors and reduced to *R* = 4.72 % and wR^2 = 14.04 % with anisotropic displacement factors. An isotropic extinction correction was applied but did not improve the final residual. The final positional and isotropic displacement parameters are given in Table 6. Bond valence sums were calculated using parameters taken from Brese & O'Keeffe (1991) and can be found in Table 7. Select bond lengths for both samples can be found in Table 8.

Overview of the structural elements

Ferraris *et al*. (1996), Ferraris (1997) and Christiansen *et al*. (1999) have described AGM and other modular titanosilicates such as bafertisite (Pen & Sheng, 1963), perraultite (Yamnova *et al*., 1998), nafertisite (Ferraris *et al*., 1996), lamprophyllite (Saf'yanov *et al*., 1983; Johnsen, 1996) and yoshimuraite (McDonald *et al*., 2000) as heterophyllosilicates. Such minerals have a *HOH* structure, where *H* = heterogeneous sheet, similar to the *TOT* structure in phyllosilicates, where TiO_5 or TiO_6 polyhedra proxy for the usual $(Si,Al)O_4$ tetrahedra in phyllosilicates. Astrophyllite group minerals are the intermediate member of a polysomatic (Ferraris *et al*., 1996) or homologous (Christiansen *et al*., 1999) series which also includes perraultite and mica as the end-member structures. A comparison of these minerals shows that they all have (1) a *HOH* structure, (2) an *a* axial length of approximately 5.4 Å, corresponding to the *a* value observed in micas, and (3) $d_{001} \approx 10.9$ Å. The homologous series can be expressed by indicating the number of diorthosilicate groups separating rows of *D* octahedra: *n* = 1 in perraultite and bafertisite, *n* = 2 in AGM, *n* = 3 in nafertisite, and *n* = ∞ in micas (modified from Ferraris *et al*., 1996 and Christiansen *et al*., 1999).

In perraultite, bafertisite, lamprophyllite and yoshimuraite, the *H*-sheet is comprised of dimers of $[Si_2O_7]^{6-}$ which are linked *via* corner-sharing to TiO_6 octahedra or TiO_5 tetragonal pyramids, resulting in a Si:Ti ratio of 2:1 The offset between successive *HOH* layers is such that the Ti are not linked across the interlayer as observed in AGM and nafertisite. In nafertisite, the *H* layer consists of open branched *zweier* double chains of $[Si_{12}O_{34}]^{20-}$ (Liebau, 1985) which are crosslinked by TiO_6 octahedra, resulting in a Si:Ti ratio of 6:1 (Ferraris *et al*., 1996).

The AGM structure can be subdivided into two main composite sheets stacked along [001] in a 2:1 ratio. The first is an *O*-sheet extending from Z ≈ 0.40 to 0.60 in triclinic species and from Z ≈ -0.05 to 0.05 in monoclinic kupletskite, consisting of a closest-packed sheet of MnO_6, FeO_6, MgO_6, or NaO_6 octahedra. There are four crystallographically distinct *O*-sheet octahedra, designated *M*(1) through *M*(4). The *O*-sheet is sandwiched between two *H*-sheets, extending from Z ≈ -0.15 to -0.05. The *H*-sheet consists of open-branched *zweier* [100] single chains of $[Si_4O_{12}]^{8-}$ (Liebau, 1985) which are in turn cross-linked by corner-sharing DO_6 octahedra, or DO_5 polyhedra as in magnesium astrophyllite (Shi *et al*., 1998), where *D* = Nb,Ti,Zr.

Table 4. Positional and displacement parameters and site occupancies for triclinic kupletskite.

Atom	*x*	*y*	*z*	*sof*	$^{*}U_{11}$	U_{22}	U_{33}	U_{23}	U_{13}	U_{12}	U_{eq}
Mn(1)	0.8500(1)	0.20620(5)	0.47875(6)	0.809(5)	89(3)	96(3)	107(3)	46(2)	17(2)	21(2)	97(2)
Na(1)	0.8500(1)	0.20620(5)	0.47875(6)	0.191(5)	89(3)	96(3)	107(3)	46(2)	17(2)	21(2)	97(2)
Mn(2)	0.27901(9)	0.06668(5)	0.48702(5)	0.974(3)	103(3)	113(3)	125(3)	57(2)	30(2)	30(2)	111(2)
Mn(3)	0.4223(1)	0.35220(5)	0.48391(5)	0.881(5)	103(3)	112(3)	133(3)	65(2)	34(2)	36(2)	110(2)
Mg(3)	0.4223(1)	0.35220(5)	0.48391(5)	0.119(5)	103(3)	112(3)	133(3)	65(2)	34(2)	36(2)	110(2)
Mn(4)	0	0.5	0.5	0.299(3)	90(5)	88(4)	105(5)	38(3)	10(3)	17(3)	97(3)
Mn(4)	0	0.5	0.5	0.201(3)	90(5)	88(4)	105(5)	38(3)	10(3)	17(3)	97(3)
Ti	0.0795(1)	0.08598(5)	0.19683(5)	0.948(4)	69(3)	94(3)	93(3)	41(2)	12(2)	21(2)	85(2)
Nb	0.0795(1)	0.08598(5)	0.19683(5)	0.052(4)	69(3)	94(3)	93(3)	41(2)	12(2)	21(2)	85(2)
Si(1)	0.6785(2)	0.27194(8)	0.23032(9)	1.00	89(4)	73(4)	86(4)	30(3)	9(3)	16(3)	86(2)
Si(2)	0.8128(2)	0.54570(8)	0.25292(9)	1.00	119(4)	85(4)	93(4)	40(3)	11(3)	15(3)	101(2)
Si(3)	0.3781(2)	0.67477(8)	0.25541(9)	1.00	119(4)	89(4)	104(4)	49(3)	12(3)	21(3)	104(2)
Si(4)	0.5081(2)	0.93072(8)	0.23432(9)	1.00	91(4)	92(4)	86(4)	48(3)	12(3)	21(3)	88(2)
K(1a)	0.1321(2)	0.2645(1)	0.9961(1)	0.885(4)							365(4)
K(1b)	0.093(3)	0.186(2)	0.998(2)	0.115(4)							365(4)
Na	0.5	0	0	0.322(6)	192(9)	122(8)	83(8)	35(5)	6(5)	25(5)	140(6)
Ca	0.5	0	0	0.178(6)	192(9)	122(8)	83(8)	35(5)	6(5)	25(5)	140(6)
O(1)	0.7290(4)	0.3203(2)	0.3824(2)	1.00	121(11)	135(11)	89(11)	37(9)	31(9)	35(9)	118(5)
O(2)	0.1483(4)	0.1593(2)	0.3675(2)	1.00	135(11)	136(11)	104(12)	35(9)	18(9)	31(9)	131(5)
O(3)	0.1292(4)	0.3949(2)	0.5948(2)	1.00	104(11)	135(11)	95(11)	38(9)	3(9)	15(8)	119(5)
OH(4)	0.2935(5)	0.4627(2)	0.3980(2)	1.00	132(11)	146(11)	147(12)	62(10)	31(9)	36(9)	142(5)
OH(5)	0.9921(4)	0.1189(2)	0.5951(2)	1.00	126(11)	155(11)	158(13)	58(10)	28(10)	32(9)	150(5)
O(6)	0.5572(4)	0.2586(2)	0.5921(2)	1.00	113(11)	124(11)	113(12)	57(9)	16(9)	23(9)	116(5)
O(7)	0.5749(4)	0.0133(2)	0.3866(2)	1.00	116(11)	150(11)	85(11)	45(9)	12(9)	42(9)	118(5)
O(8)	0.0724(4)	0.5917(2)	0.2007(2)	1.00	143(12)	223(13)	137(13)	72(10)	20(10)	-19(10)	182(6)
O(9)	0.2460(5)	0.0417(3)	0.8296(3)	1.00	215(13)	246(14)	158(14)	25(11)	62(11)	-78(11)	250(6)
O(10)	0.4319(5)	0.4153(2)	0.7994(2)	1.00	196(12)	202(12)	141(13)	60(10)	15(10)	118(10)	174(5)
O(11)	0.1297(6)	0.8100(3)	0.8330(3)	1.00	352(15)	295(14)	184(14)	115(12)	100(12)	253(12)	240(6)
O(12)	0.2646(5)	0.9567(3)	0.1693(3)	1.00	294(14)	228(13)	157(13)	23(11)	-72(11)	170(11)	236(6)
O(13)	0.2665(5)	0.6074(2)	0.8089(2)	1.00	292(14)	102(11)	136(12)	50(9)	14(11)	16(10)	186(6)
O(14)	0.5721(5)	0.2222(2)	0.8031(3)	1.00	314(14)	109(11)	175(13)	84(10)	48(11)	41(10)	195(6)
O(15)	0.3807(5)	0.1906(3)	0.1672(3)	1.00	159(12)	310(15)	167(14)	119(12)	-37(10)	-106(11)	241(6)
F(16)	0	0	0	0.50	37(13)	67(13)	52(14)	27(11)	3(11)	31(10)	49(6)

$^{*}U$ij x 10^4 Å

Table 5. Empirical bond-valences (*v.u.*) for triclinic kupletskite.

	A (1a)	*A* (1b)	*B*	*M* (1)	*M* (2)	*M* (3)	*M* (4)	*D*	*T* (1)	*T* (2)	*T* (3)	*T* (4)	Σ
O(1)				0.294		0.383	0.358$\downarrow^{X2}$		1.005				2.090
O(2)				0.342	0.278	0.290		1.038					1.948
O(3)				0.318		0.364	0.337$\downarrow^{X2}$			1.027			2.046
OH(4)						0.698	0.407$\downarrow^{X2}$						1.105
OH(5)				0.334	0.763								1.097
O(6)				0.339	0.303	0.348					1.027		2.017
O(7)				0.319	0.687							0.995	2.001
O(8)	0.017									0.953	0.953		1.923
O(9)	0.126	0.022	0.140$\downarrow^{X2}$					0.693				1.039	2.020
O(10)	0.024									0.953	0.960		1.937
O(11)	0.127	0.023	0.137$\downarrow^{X2}$					0.687	1.036				2.010
O(12)	0.131	0.023	0.138$\downarrow^{X2}$					0.689				1.030	2.011
O(13)	0.053								0.935	1.030			2.018
O(14)	0.055										1.036	0.958	2.049
O(15)	0.130	0.022	0.135$\downarrow^{X2}$					0.689	1.033				2.009
ϕ(16)	0.065$\rightarrow^{X3}$	0.030$\rightarrow^{X3}$	0.076$\downarrow^{X2}\rightarrow$					0.428$\rightarrow^{X2}$					1.198
Σ	0.728	0.120	1.252	1.946	2.031	2.083	2.204	4.224	4.009	3.963	3.976	4.022	

* constants from Brese & O'Keeffe (1991)

Table 6. Positional and displacement parameters and site occupancies for monoclinic kupletskite.

Atom	*x*	*y*	*z*	*sof*	$^{*}U_{11}$	U_{22}	U_{33}	U_{23}	U_{13}	U_{12}	U_{eq}
Mn(1)	0.2527(1)	0.39265(3)	0.00989(3)	0.913(7)	94(4)	88(4)	134(4)	-2(4)	17(2)	0(5)	105(2)
Na(1)	0.2527(1)	0.39265(3)	0.00989(3)	0.087(7)	94(4)	88(4)	134(4)	-2(4)	17(2)	0(5)	105(2)
Mn(2)	0.7461(1)	0.03613(3)	-0.00589(3)	0.990(3)	92(4)	86(4)	158(4)	13(3)	28(3)	-3(4)	111(2)
Mn(3)	0.7468(1)	0.17930(3)	-0.00728(3)	0.966(4)	95(4)	92(4)	150(4)	6(4)	35(3)	9(5)	111(2)
Mn(4)	0.25	0.25	0	0.431(4)	95(6)	91(5)	140(5)	-18(5)	6(4)	2(5)	109(3)
Mg(4)	0.25	0.25	0	0.069(4)	95(6)	91(5)	140(5)	-18(5)	6(4)	2(5)	109(3)
Ti	-0.4641(1)	0.10716(3)	-0.15196(3)	0.881(4)	77(3)	130(3)	145(4)	-17(3)	12(2)	-5(3)	117(2)
Nb	-0.4641(1)	0.10716(3)	-0.15196(3)	0.119(4)	77(3)	130(3)	145(4)	-17(3)	12(2)	-5(3)	117(2)
Si(1)	0.0417(2)	0.19281(5)	-0.13490(6)	1.00	85(6)	101(6)	113(6)	27(4)	6(4)	4(4)	100(3)
Si(2)	0.0391(2)	0.32547(5)	-0.12427(6)	1.00	167(6)	107(6)	112(6)	1(5)	11(4)	-3(5)	129(3)
Si(3)	0.9601(2)	0.11053(5)	0.12310(6)	1.00	154(6)	101(5)	113(5)	6(5)	13(4)	-7(5)	123(2)
Si(4)	1.0417(2)	0.02169(5)	-0.13312(6)	1.00	114(6)	75(6)	105(6)	2(4)	11(4)	1(4)	98(3)
K(1)	-0.5	0.24270(9)	-0.25	0.50	568(13)	495(12)	285(10)	0	20(9)	0	451(5)
K(2)	0.5	-0.02746(9)	-0.25	0.50	579(13)	416(11)	280(10)	0	31(9)	0	425(5)
Na	-1.0	0.10683(8)	-0.25	0.301(7)	266(11)	142(10)	75(9)	0	5(6)	0	162(6)
Ca	-1.0	0.10683(8)	-0.25	0.199(7)	266(11)	142(10)	75(9)	0	5(6)	0	162(6)
O(1)	0.0676(5)	0.1842(2)	-0.0582(1)	1.00	109(15)	121(17)	88(14)	-8(13)	-5(12)	-4(15)	107(7)
O(2)	0.5672(5)	0.1077(2)	-0.0655(1)	1.00	117(14)	119(14)	113(14)	-1(15)	1(11)	-8(15)	117(6)
O(3)	0.0672(5)	0.3234(2)	-0.0474(1)	1.00	86(15)	140(16)	100(14)	-19(15)	14(11)	-12(16)	108(6)
OH(4)	-0.0652(6)	0.2477(2)	0.0505(1)	1.00	117(16)	152(16)	163(16)	-36(15)	42(13)	3(16)	142(7)
OH(5)	0.4343(6)	0.0391(2)	0.0474(1)	1.00	139(17)	123(17)	188(17)	-11(16)	23(13)	-7(16)	150(7)
O(6)	0.9289(5)	0.1094(2)	0.0457(1)	1.00	129(14)	109(14)	109(14)	-14(16)	17(11)	-14(16)	115(6)
O(7)	1.0664(5)	0.0309(2)	-0.0563(1)	1.00	126(16)	127(17)	104(15)	-10(13)	17(12)	-7(15)	119(7)
O(8)	0.2753(7)	0.3593(1)	-0.1507(2)	1.00	337(21)	335(20)	154(18)	12(15)	4(15)	-174(17)	277(9)
O(9)	-0.7252(6)	0.0491(2)	-0.1645(2)	1.00	315(20)	385(22)	179(18)	-58(16)	95(16)	-208(17)	289(9)
O(10)	-0.2240(7)	0.3557(2)	-0.1510(2)	1.00	339(21)	360(21)	174(19)	41(15)	27(16)	207(17)	291(9)
O(11)	0.2749(6)	0.1660(2)	-0.1663(2)	1.00	313(20)	380(22)	175(18)	28(16)	81(15)	200(17)	286(9)
O(12)	0.7863(6)	0.0486(2)	-0.1655(2)	1.00	296(20)	353(21)	203(18)	-59(16)	-66(15)	207(16)	289(9)
O(13)	0.0367(7)	0.2615(1)	-0.1542(2)	1.00	431(22)	107(15)	164(16)	-10(13)	8(15)	-7(15)	235(8)
O(14)	0.9628(7)	0.0464(1)	0.1523(2)	1.00	486(23)	115(16)	172(17)	32(13)	27(16)	1(15)	258(8)
O(15)	-0.2133(6)	0.1660(2)	-0.1666(2)	1.00	279(19)	382(22)	178(18)	68(16)	-75(15)	-195(17)	285(9)
F(16)	-0.5	0.1064(2)	-0.25	0.50	222(19)	264(20)	172(19)	0	2(15)	0	220(8)

$^{*}U$ij x 10^4 Å

Table 7. Empirical bond-valences (*v.u.*) for monoclinic kupletskite.

	A(1)	*A*(2)	*B*	*M*(1)	*M*(2)	*M*(3)	*M*(4)	*D*	*T*(1)	*T*(2)	*T*(3)	*T*(4)	Σ
O(1)				0.302		0.388	0.370↓^{X2}		0.984				2.044
O(2)				0.351	0.284	0.288		1.013					1.936
O(3)				0.332		0.375	0.347↓^{X2}			1.003			2.057
OH(4)						0.712	0.427↓^{X2}						1.139
OH(5)				0.343	0.790								1.133
O(6)				0.357	0.321	0.357					0.976		2.011
O(7)				0.320	0.714							0.973	2.007
O(8)										0.960	0.930		1.890
O(9)		0.130↓^{X2}	0.139↓^{X2}					0.717				1.044	2.030
O(10)										0.960	0.927		1.887
O(11)	0.139↓^{X2}		0.141↓^{X2}					0.686	1.058				2.024
O(12)		0.137↓^{X2}	0.143↓^{X2}					0.705				1.039	2.024
O(13)	0.064↓^{X2}								0.937	1.027			2.028
O(14)		0.031↓^{X2}									1.030	0.979	2.040
O(15)	0.138↓^{X2}		0.145↓^{X2}					0.683	1.061				2.027
ϕ(16)	0.061→^{X2}	0.071→^{X2}	0.077↓^{X2}→					0.461→^{X2}					1.340
Σ	0.743	0.667	1.320	2.005	2.109	2.031	2.288	4.265	4.040	3.950	3.863	4.035	

* constants from Brese & O'Keeffe (1991)

Table 8. Select bond length (Å) for triclinic and monoclinic kupletskite.

$P\bar{1}$		$C2/c$		$P\bar{1}$		$C2/c$	$P\bar{1}$		$C2/c$
A		***A*(1)**		***M*(1)O$_5$(OH) octahedron**			***D*ϕ_6 octahedron**		
K(1a)-O(12)	2.836(3)	K(1)-O(11)	2.861(4)	*M*(1)-O(2)	2.189(2)	2.178(3)	*D*-O(2)	1.807(3)	1.823(3)
K(1a)-O(15)	2.839(3)	K(1)-O(11)	2.861(4)	*M*(1)-O(5)	2.198(3)	2.187(4)	*D*-O(12)	1.959(3)	1.957(3)
K(1a)-O(11)	2.847(3)	K(1)-O(15)	2.863(4)	*M*(1)-O(6)	2.191(2)	2.172(3)	*D*-O(11)	1.960(3)	1.967(3)
K(1a)-O(9)	2.852(3)	K(1)-O(15)	2.863(4)	*M*(1)-O(3)	2.216(2)	2.199(4)	*D*-O(9)	1.956(2)	1.951(3)
K(1a)-ϕ(16)	3.093(1)	K(1)-ϕ(16)	3.167(4)	*M*(1)-O(7)	2.214(2)	2.213(4)	*D*-O(15)	1.959(3)	1.969(3)
K(1a)-O(14)	3.399(3)	K(1)-O(13)	3.391(4)	*M*(1)-O(1)	2.244(2)	2.234(4)	*D*-ϕ(16)	2.084(1)	2.068(1)
K(1a)-O(13)	3.429(3)	K(1)-O(13)	3.391(4)	<*M*(1)-O>	2.209	2.197	<*D*-ϕ>	1.954	1.956
K(1a)-O(14)	3.429(3)	K(1)-O(13)	3.411(4)						
K(1a)-O(13)	3.442(3)	K(1)-O(13)	3.411(4)	***M*(2)O$_4$(OH)$_2$ octahedron**			***T*(1) tetrahedron**		
K(1a)-O(8)	3.606(3)	<K(1)-ϕ>	3.135	*M*(2)-O(7)	2.128(2)	2.118(3)	*T*(1)-O(15)	1.612(3)	1.602(3)
K(1a)-O(10)	3.699(3)			*M*(2)-O(5)	2.130(2)	2.112(3)	*T*(1)-O(11)	1.611(3)	1.603(3)
K(1a)-O(10)	3.705(3)	***A*(2)**		*M*(2)-O(5)	2.144(2)	2.149(4)	*T*(1)-O(1)	1.622(3)	1.630(3)
<K(1a)-ϕ>	3.265	K(2)-O(12)	2.866(4)	*M*(2)-O(6)	2.222(2)	2.207(4)	*T*(1)-O(13)	1.649(3)	1.648(3)
		K(2)-O(12)	2.866(4)	*M*(2)-O(7)	2.231(2)	2.224(4)	<*T*(1)-O>	1.624	1.621
K(1b)-ϕ(16)	2.176(18)	K(2)-O(9)	2.866(4)	*M*(2)-O(2)	2.254(3)	2.252(4)			
K(1b)-O(15)	2.392(18)	K(2)-O(9)	2.886(4)	<*M*(2)-O>	2.185	2.177	***T*(2) tetrahedron**		
K(1b)-O(11)	2.397(18)	K(2)-ϕ(16)	3.108(4)				*T*(2)-O(13)	1.613(2)	1.614(3)
K(1b)-O(12)	2.392(17)	K(2)-O(14)	3.417(4)	***M*(3)O$_4$(OH)$_2$ octahedron**			*T*(2)-O(3)	1.614(3)	1.623(3)
K(1b)-O(9)	2.407(17)	K(2)-O(14)	3.417(4)	*M*(3)-O(1)	2.135(2)	2.127(3)	*T*(2)-O(8)	1.642(3)	1.639(4)
<K(1b)-ϕ>	2.353	<K(2)-ϕ>	3.064	*M*(3)-O(4)	2.137(3)	2.124(4)	*T*(2)-O(10)	1.642(3)	1.639(4)
				M(3)-O(3)	2.153(2)	2.140(3)	<*T*(2)-O>	1.628	1.629
***B*ϕ_{10} polyhedra**				*M*(3)-O(6)	2.170(2)	2.158(4)			
B-O(12)x2	2.599(3)	2.596(4)		*M*(3)-O(4)	2.204(2)	2.198(4)	***T*(3) tetrahedron**		
B-O(9)x2	2.596(3)	2.606(4)		*M*(3)-O(2)	2.237(2)	2.238(4)	*T*(3)-O(14)	1.611(3)	1.613(3)
B-O(11)x2	2.604(3)	2.600(4)		<*M*(3)-O>	2.173	2.164	*T*(3)-O(6)	1.614(3)	1.633(3)
B-O(15)x2	2.610(3)	2.590(4)					*T*(3)-O(10)	1.639(3)	1.652(4)
B-ϕ(16)x2	2.696(0)	2.701(0)		***M*(3)O$_4$(OH)$_2$ octahedron**			*T*(3)-O(8)	1.642(2)	1.651(3)
<*B*-ϕ>	2.621	2.619		*M*(4)-O(4)x2	2.087(2)	2.093(3)	<*T*(3)-O>	1.627	1.637
				M(4)-O(1)x2	2.135(2)	2.146(4)			
				M(4)-O(3)x2	2.156(2)	2.170(4)	***T*(4) tetrahedron**		
				<*M*(4)-O>	2.126	2.136	*T*(4)-O(9)	1.610(3)	1.608(3)
							T(4)-O(12)	1.613(3)	1.610(3)
							T(4)-O(7)	1.626(3)	1.634(3)
							T(4)-O(14)	1.640(3)	1.632(3)
							<*T*(4)-O>	1.622	1.621

The resultant Si:Ti ratio is 4:1. Individual *D*O$_6$ octahedra are linked across the interlayer *via* a common apical anion [ϕ(16), where ϕ = unspecified anion]. The interlayer of triclinic AGM contains two crystallographically distinct cation sites, *A* and *B*, whereas kupletskite-*Ma*2*b*2*c* contains three crystallographically distinct cation sites, *A*1, *A*2 and *B*. The variation in stacking sequence of individual *HOH* layers is responsible for the polytypism observed between monoclinic and triclinic kupletskite.

Polytypism in the astrophyllite group

By definition, a mineral is polytypic if it occurs in several structural modifications which are related to each other by stacking of layers identical in structure and composition such that differences in the structural states are due only to differences in stacking sequences (Bailey *et al*., 1978; Guinier *et al*., 1984; Nickel & Grice, 1998). Polytypism in the astrophyllite group has been proposed by a number of workers and recognized in electron diffraction studies (Vrublevskaya & Zvyagin, 1976; Zvyagin & Vrublevskaya, 1976; Dornberger-Schiff *et al*., 1985; Christiansen *et al*., 1999). The basis for the theoretical derivation of 14 modular polytypic AGM structures by Zvyagin & Vrublevskaya (1976), and later by Dornberger-Schiff *et al*. (1985), was that of "building layers" or "modules", each consisting of a combination of two neighboring *H*-sheets linked *via* a common apical anion, and an independent *O*-sheet. In such an approach, a

centered orthogonal cell defined by two octahedra wide (*a*) and seven octahedra long (*b*) is used. The base of each of seven *O*-sheet octahedra is regarded as a regular triangular network of anions, resulting in seven possible attachment points for the adjacent *H-H* layer. The mutual disposition of the *H-H* units over apical positions (*HHO* units) results in four geometrically different *HHOHH* units and 14 possible polytypes with either triclinic, monoclinic or orthorhombic symmetry (Zvyagin & Vrublevskaya, 1976). Four of these 14 derived structures are based on the same triclinic subcell as the present polytype pair. Only three of these arrangements have been found in nature: monoclinic magnesium astrophyllite (#1; Peng & Ma, 1963; Shi *et al.*, 1998), triclinic AGM (#3; Woodrow, 1967; Christiansen *et al.*, 1998; Piilonen *et al.*, 2000), and kupletskite-*Ma*2*b*2*c* (#6). It should be noted that monoclinic magnesium astrophyllite and the other triclinic members of the astrophyllite group should not be considered to be polytypic derivatives of each other – structurally and chemically, magnesium astrophyllite is distinctly different in that the *H*-sheet contains [5]-coordinated TiO_5 polyhedra and the *O*-sheet hosts significant amounts of Na and Mg.

Possible crystallographic mechanisms for the formation of astrophyllite group polytypes include cation ordering, changes in packing of coordinating anions, variations in orientation of the *O*-sheet octahedra with respect to the adjacent *H*-sheets, as is observed in lamprophyllite-2*M* and lamprophyllite-2*O* (Johnsen, 1996), or by complete translation of the *HOH* layer by combinations of symmetry elements not evidenced in the triclinic structure. Since the minerals of the astrophyllite group are defined as layered silicates composed of *HOH* layers that are similar to the *TOT* layers in mica, the present polytype pair can similarly be described as variations in the stacking of *HOH* layers. As such, the "building layer" chosen for this study is the *HOH* layer.

The structural make-up of the *HOH* layers in triclinic and monoclinic kupletskite differs only in the designation of the single, albeit split, *A* site in triclinic species as *A*(1) and *A*(2) in the monoclinic species. In all other aspects, individual *HOH* layers are structurally identical. Chemically, the two samples differ only slightly in Mn/(Mn+Fe): 0.87 (triclinic), and 0.66 (monoclinic). Triclinic kupletskite (RUS12) also shows a slight enrichment in Na, Mg and depletion in Nb and Al with respect to monoclinic kupletskite (RUS9).

In the triclinic structure (Fig. 1), adjacent *HOH* layers are related to each other by a center of symmetry. Stacking can thus be described as either +*HOH*/+*HOH*/+*HOH*, or simply +++, with a layer-stacking period of one. This polytypic form is

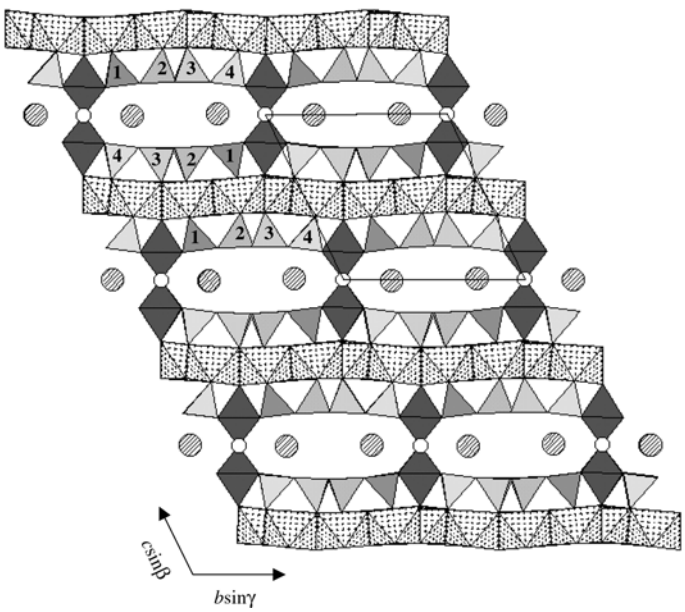

Fig. 1. Crystal structure of triclinic, $P\bar{1}$, kupletskite projected down [100] (unit cell outlined). *A* = hatched, *B* = white, *O*-sheet = stippled, *D* = dark gray, *T*(1) to *T*(4) = medium gray to light gray. The four *T* sites are numbered to illustrate the symmetry across the interlayer.

equivalent to #3 derived by Zvyagin & Vrublevskaya (1976). A displacement of ≈ 5 Å along *b* exists between adjacent layers, resulting in an offset of the adjacent layers such that the apices of the $D\phi_6$ octahedra do not define an orthogonal arrangement.

In monoclinic kupletskite (Fig. 2), adjacent *HOH* layers are related by a two-fold axis parallel to *b*, resulting in a stacking period along *c* of two differently oriented *HOH* layers herein defined as *+HOH* and *–HOH*. In this way, neither attachment points of the *H*-sheet nor first neighbor coordination spheres are compromised, and the *HOH* layer is geometrically to that observed in triclinic species. The resulting stacking sequence with a two-layer period can be described as *+HOH*/*–HOH*/*+HOH*, or simply +–+–. This polytypic form is equivalent to #6 derived by Zvyagin & Vrublevskaya (1976). A more orthogonal configuration is achieved such that *D*-ϕ(16)-*D* polyhedral pairs lie in planes perpendicular to (001). The resultant relationship between the unit cell parameters of monoclinic and triclinic kupletskite are as follows: $a_{monoclinic} = a_{triclinic}$, $b_{monoclinic} = 2(b\sin\gamma)_{triclinic}$, and $c_{monoclinic}$ spans two *HOH* layers. Figure 3 depicts the stacking sequence differences between the two polytypes.

In accordance with IMA guidelines for the nomenclature of polytypes, triclinic varieties of kupletskite should be referred to as kupletskite-1*A*. Monoclinic species, in which both the *b* and *c* parameters extend over two periods respect to the triclinic primitive subcell, should be referred to as kupletskite-*Ma*2*b*2*c* (Bailey *et al*., 1978; Nickel & Grice, 1987).

Discussion

As with other 1:1 and 2:1 phyllosilicates, the physical and/or crystal chemical mechanisms responsible for polytype formation in AGM are unknown. A study of 21 AGM from both over- and undersaturated intrusions (P. Piilonen unpublished data) revealed only one monoclinic modification (kupletskite-*Ma*2*b*2*c*), suggesting that triclinic AGM are energetically more favorable under a wide range of crystallization conditions. The presence of a split *A* site in the kupletskite-1*A*, a feature common to other triclinic AGM, and the lack of such disorder in kupletskite-*Ma*2*b*2*c* may also suggest that kupletskite-1*A* is more stable than that of the monoclinic polytype.

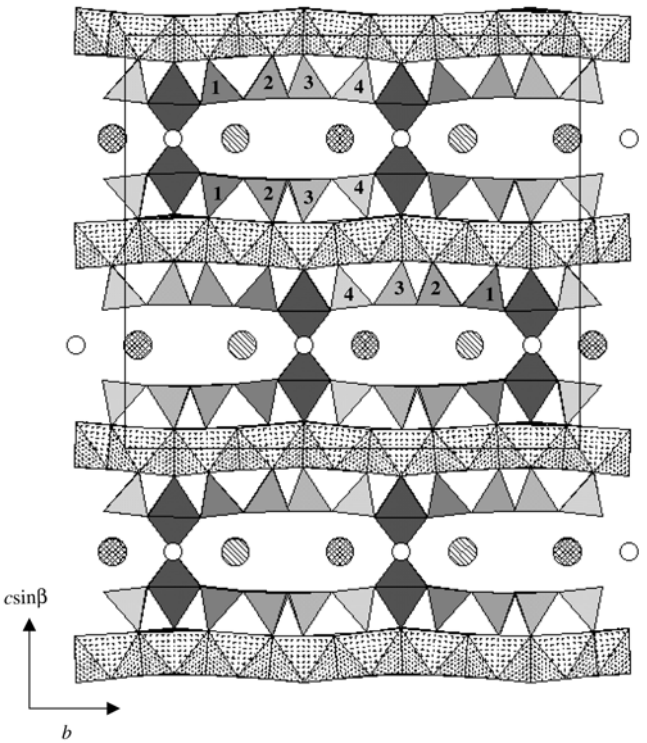

Fig. 2. Crystal structure of monoclinic, *C*2/*c*, kupletskite, projected down [100] (unit cell outlined). *A*(1) = hatched, *A* (2) = diagonal lines, *B* = white, *O*-sheet = stippled, *D* = dark gray, *T*(1) to *T*(4) = medium gray to light gray. The four *T* sites are numbered to illustrate the symmetry across the interlayer.

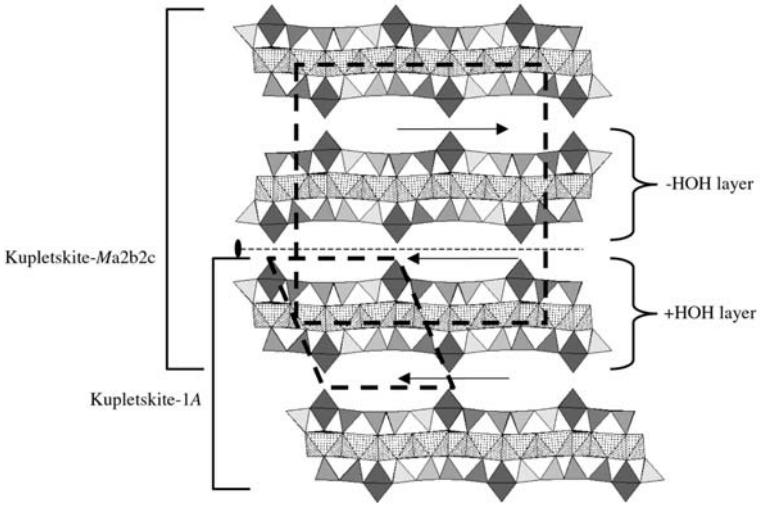

Fig. 3. Monoclinic and triclinic kupletskite polytypes projected down [100]. Unit cells for both structures are outlined. In kupletskite–*Ma2b2c*, *+HOH* and *–HOH* layers are related to each other by the two-fold rotation around *b*. Arrows depict stacking sequence.

It has been suggested (Zvyagin & Vrublevskaya, 1976) that the degree of uniformity in the distribution of DO_6 or DO_5 polyhedra may be responsible for the formation of AGM polytypes. Attachment of Ti cations to the *O*-sheet results in an imbalance in charge distribution and bond valence associated with the O(2) apical oxygen and the three octahedral sites to which it is bonded, *M*(1), *M*(2) and *M*(3); the most favorable arrangement of Ti cations is such that this imbalance is distributed uniformly over the entire structure so as to avoid charge overloading. In monoclinic magnesium astrophyllite, DO_5 polyhedra are related by a two-fold axis and are located on either side of the *M*(1) octahedron in planes parallel to [001]. As a result, two of the oxygens coordinating the *M*(1) octahedron are underbonded. This charge imbalance is accounted for by the dominance of Na, a large monovalent cation, in *M*(1). In triclinic modifications of AGM, the DO_6 polyhedra are uniformly distributed such that charge imbalance is minimized and does not occur repeatedly in any given part of the structure. In kupletskite-*Ma2b2c*, the distribution of DO_6 octahedra is closer to that observed in triclinic species: pairs of octahedra in alternate layers are located in planes perpendicular to (001), resulting in only partial uniformity and therefore long-range overloading of electrical charge on the *O*-sheet octahedra. Unlike magnesium astrophyllite, kupletskite-*Ma2b2c* does not have a dominance of Na in *M*(1) to overcome this charge imbalance.

The high *R* values (> 4.0 %) observed in many of the structure refinements, coupled with extensive streaking observed in precession photographs, suggest the possibility of additional polytypic intergrowths or stacking disorder in the astrophyllite group, in agreement with electron diffraction studies performed by Zvyagin & Vrubleskaya (1976). Further work by high resolution TEM may be required to elucidate these problems.

Acknowledgements: The authors thank Mr. M. Cooper and Dr. F.C. Hawthorne of the Department of Geological Sciences, University of Manitoba, for use of the 4-circle X-ray diffractometer, Mr. L. Horváth for providing the sample from Mount Kuivchorr, Mr. D. Belakovskiy of the Moscow Mineralogical Museum for providing a sample of holotype kupletskite, Mr. R.A. Gault of the Canadian Museum of Nature for the electron microprobe analyses, and Dr. T.S. Ercit for insightful discussions. The comments by Mr. C.C. Christiansen, an anonymous review, an associate editor and Dr. A. Mottana are greatly appreciated. Financial support was provided by the Natural Sciences and Engineering Research Council of Canada in the form of a scholarship to PCP and grants to AMM and AEL, and by the University of Ottawa and Laurentian University.

References

Bailey, S.W., Frank-Kamenetskii, V.A., Goldsztaub, S., Kato, A., Pabst, A., Schultz, H., Taylor, H.F.W., Fleischer, M., Wilson, A.J.C. (1978): Report of the International Mineralogical Association (IMA)-International

Union of Crystallography (IUCr) Joint Committee on nomenclature. *Can. Mineral*., **16**, 113-117.

Brese, N.E. & O'Keeffe, M. (1991): Bond-valence parameters for solids. *Acta Crystallogr*., **B47**, 192-197.

Brooks, C.K., Engell, J., Larsen, L.M., Pedersen, A.K. (1982): Mineralogy of Werner Bjerge alkaline complex, East Greenland. *Meddelelser om Grønland, Geoscience*, **7**, 38 pp.

Bruker Analytical X-Ray Systems (1997): XPREP - Data preparation and Reciprocal Space Exploration.

Christiansen, C.C., Johnsen, O., Ståhl, K. (1998): Crystal structure of kupletskite from the Kangerdlugssuaq intrusion, East Greenland. *N. Jahrb. Mineral. Monatsh.*, **1998**, 253-264.

Christiansen, C.C., Makovicky, E., Johnsen, O. (1999): Homology and typism in heterophyllosilicates: An alternative approach. *N. Jahrb. Mineral. Abh*., **175**, 153-189.

DeMark, R.S. (1984): Minerals of Point of Rocks, New Mexico. *Mineral. Rec.*, **15**, 149-156.

Dornberger-Schiff, K., Drits, V.A., Durovic, S., Zvyagin, V.V. (1985): Special form of polytypism potentially occurring in astrophyllite structures. *Sov. Phys. Crystallogr*., **30**, 292-294.

Ferraris, G. (1997): Polysomatism as a tool for correlating properties and structure. *In* EMU Notes in Mineralogy: Modular aspects of minerals. **1**, 275-295.

Ferraris, G., Ivaldi, G., Khomyakov, A.P., Soboleva, S.V., Belluso, E., Pavese, A. (1996): Nafertisite, a layer titanosilicate member of a polysomatic series including mica. *Eur. J. Mineral*., **8**, 241-249.

Guinier, A., Bokij, G.B., Boll-Dornberger, K., Cowley, J.M., Ďurovič, S., Jagodzinski, H., Krishna, P., deWolff, P.M., Zvyagin, B.B., Cox, D.E., Goodman, P., Hahn, T., Kuchitsu, K., Abrahams, S.C. (1984): Nomenclature of polytype structures – Report of the International Union of Crystallography Ad-Hoc Committee on the nomenclature of disordered, modulated and polytype structures. *Acta Cryst.*, **A40**, 399-404.

Horváth, L. & Gault, R.A. (1990): The mineralogy of Mont Saint-Hilaire, Québec. *Mineral. Rec*., **21**, 284-359.

Johnsen, O. (1996): TEM observations and X-ray powder data on lamprophyllite polytypes from Gardiner Complex, East Greenland. *N. Jahrb. Mineral. Monatsh*., **1996**, 407-417.

Liebau, F. (1985): Structural Chemistry of Silicates: Structure, Bonding and Classification. Springer-Verlag, Berlin.

McDonald, A.M., Grice, J.D., Chao, G.Y. (2000): The crystal structure of yoshimuraite, a layered Ba-Mn-Ti silicophosphate, with comments on five-coordinated Ti^{4+}. *Can. Mineral*., **38**, 649-656.

Nickel, E.H. & Grice, J.D. (1998): The IMA Commission on New Minerals and Mineral Names: Procedures and guidelines on mineral nomenclature. *Can. Mineral*., **36**, 913-926.

Pen, Z.Z. & Sheng, T.C. (1963): Crystal structure of bafertisite, a new mineral from China. *Sci. Sinica*., **12**, 278-280.

Peng, C.C. & Ma, C.S. (1963): Crystal structure of astrophyllite and a new type of band silicate radical. *Sci. Sinica*., **12**, 272-276.

Piilonen, P.C., Lalonde, A.E., McDonald, A.M., Gault, R.A. (2000): Niobokupletskite, a new astrophyllite-group mineral from Mont Saint-Hilaire, Québec, Canada: Description and crystal structure. *Can. Mineral*., **38**, 627-639.

Raade, G. & Haug, J. (1982): Gjerdingen – Fundstelle seltener Mineralien in Norwegen. *Lapis*, **7**, 9-15.

Saf'yanov, Y.N., Vasil'eva, N.O., Golovachev, V.P., Kuz'min, É.A., Belov, N.V. (1983): Crystal structure of lamprophyllite. *Sov. Phys. Crystallogr.*, **28**, 207-209.

Semenov, E.I. (1956): Kupletskite – a new mineral of the astrophyllite group. *Dokl. Akad. Nauk. SSSR*., **108**, 933-936.

Sheldrick, G.M. (1993): SHELXL-93. Program for the refinement of crystal structures. University of Göttingen, Germany.

Shi, N., Ma, Z., Li, G., Yamnova, N.A., Pushcharovsky, D.Y. (1998): Structure refinement of monoclinic astrophyllite. *Acta Cryst.*, **B54**, 109-114.

Valter, A.A., Eryomenko, G.K., Leesenko, T.A. (1965): Kupletskite from the alkaline rocks of the Azov Region. *Min. Sborn*., **19**, 248-252.

Vrublevskaya, Z.V. & Zvyagin, B.B. (1976): Diffraction characteristics of polytypic forms of astrophyllite. *Sov. Phys. Crystallogr*., **21**, 546-549.

Woodrow, P.J. (1967): The crystal structure of astrophyllite. *Acta Cryst.*, **22**, 673-678.

Wooley, A.R. & Platt, G.R. (1988): The peralkaline nepheline syenites of the Junguni intrusion, Chilwa province, Malawi. *Mineral. Mag*., **52**, 425-433.

Yamnova, N.A., Egorov-Tismenko, Yu.K., Pekov, I.V. (1998): Crystal structure of perraultite from the Coastal Region of the Sea of Azov. *Crystallogr. Rep*., **43**, 401-410.

Zvyagin, B.B. & Vrublevskaya, Z.V. (1976): Polytypic forms of astrophyllite. *Sov. Phys. Crystallogr*., **21**, 542-545.

Received 20 November 2000
Modified version received 24 March 2001
Accepted 24 April 2001